PAPER • OPEN ACCESS

Numerical study of the Thermo-hydrodynamic behavior of a non-Newtonian nanofluid in a backward facing step

To cite this article: A. Mokhefi *et al* 2024 *J. Phys.: Conf. Ser.* **2685** 012074

View the article online for updates and enhancements.

Numerical study of the Thermo-hydrodynamic behavior of a non-Newtonian nanofluid in a backward facing step

A. Mokhefi[1], E. Rossi di Schio[2,*], P. Valdiserri[2], C. Biserni[2] and D. Derbal[1]

[1]Mechanics, Modeling and Experimentation Laboratory L2ME, Faculty of Sciences and Technology, Bechar University, B.P.417, 08000, Bechar, ALGERIA.
[2]Alma Mater Studiorum – University of Bologna, Department of Industrial Engineering DIN. Viale Risorgimento 2, I-40136 Bologna, ITALY.

* Corresponding author: eugenia.rossidischio@unibo.it

Abstract. In the present work, a numerical simulation of a laminar non-isothermal flow of a non-Newtonian nanofluid in a backward facing step (BFS) is presented. It deals with Cu-water nanofluid, where the mixture shows a shear thinning behavior flowing from the restricted part of the duct with a fully developed velocity and a cold temperature. The lower part of the extended area of the backward facing step is maintained at a hot temperature, while all the other boundaries are considered thermally insulated. Moreover, a uniform magnetic field according to different angle is applicated on the nanofluid flow. The numerical simulation is based on the resolution of the mass, momentum and energy balance equations using Comsol Multiphysics. The aim of the sensitivity study is to highlight the impact of the Reynolds number, the nanoparticles concentration, the Hartmann number and the angle of the magnetic field on the flow and the thermal behaviours, as well as on the Nusselt number. Surprisingly, the results show that an increase in the Hartmann number, corresponding to a more intense magnetic field, resulted in a significant reduction in flow intensity.

1. Introduction

The Backward Facing Step (BFS), also known as a backward step, is a geometric configuration commonly studied in fluid mechanics due to its many engineering applications. In fact, studies on the BFS help to better understand flow characteristics in real-life situations such as flow around vehicles, cooling systems, pipelines and heat exchangers. This configuration provides valuable insights into phenomena like boundary layer separation, vortices, unsteady flows, turbulence, and heat transfer. The sudden expansion in BFS causes the separation and reattachment of flows, and this expansion is a determining factor in the hydrodynamic structure of the flow, which has a significant impact on heat transfer. Certainly, the separation and reattachment of the flow at a backward-facing step have garnered significant attention, leading to numerous studies dedicated to this phenomenon [1-4]. To achieve a more precise forecast of flow behavior, it is essential to thoroughly describe fluid parameters and accurately identify the rheological consequences involved. Mahmoud et al. [5] employed the finite element method to examine the flow behavior of Newtonian fluids as well as power law fluids that exhibit shear thinning or thickening characteristics. Many researchers are focused on improving heat transfer to meet the demands of various processes. To enhance convective heat transfer, a novel approach has emerged, which involves the introduction of nanoparticles into the base fluid. In recent studies, researchers have conducted several investigations to demonstrate the efficacy of utilizing nanoparticles in base fluids [6-7]. Selimefendigil et al. [8] examined the impact of nanoparticles' volume fraction, inlet oscillation frequency, and Reynolds number on fluid flow and thermal transfer characteristics. Their findings revealed that heat transfer was enhanced with higher volume fractions

of nanoparticles, increased Reynolds numbers, and frequencies of oscillation. Through experimental analysis, they observed that the degree of heat transfer in a backward-facing step duct increased as the concentration of nanoparticles in the fluid rose. In their numerical study, Selimefendigil and Öztop [9] investigated the forced convection heat transfer in a backward-facing step duct with a baffle positioned on the top wall under pulsating laminar flow conditions. The researchers examined the influence of various crucial parameters and compared the results to a steady flow without a baffle. Their findings indicated that, in the scenario where the lower wall was located downstream of the enlargement, the presence of a deflector did not yield significant improvements in heat transfer. Selimefendigil et al. [10] examined the laminar forced convection of a pulsed nanofluid flow over a backward-facing step (BES). that the rate of heat transfer increased with the addition of nanoparticles in the nanofluid.

The novelty of the present analysis is the investigation of the effect of a magnetic field, with different possible angles, applied to the nanofluid flow facing, in fully developed forced convection regime, the BFS.

2. Problem description

The study domain is a Backward Facing Step (BFS), reduced in two-dimensional geometry as shown in figure 1. The water-CuO nanofluid displaying a shear-thinning behavior flows from the narrowed part of the Backward Facing Step with a fully developed velocity profile of maximum U_0 and a fully cold temperature (T_c). In addition, the lower wall of the widened portion is maintained at a hot temperature (T_h). On the other hand, the other walls of the BFS are considered thermally insulated. The flow of the nanofluid inside the BFS is subject to a magnetic field of uniform flux density B, described by an angle γ between the magnetic field B and the horizontal axis.

The thermophysical properties of the studied nanoparticles and base fluid are shown in Table 1.

According to the values of the volume fraction of the nanoparticles, the values of the non-Newtonian water-CuO nanofluid consistency as well as the index of the pseudoplastic behavior *n* are experimentally determined and shown in Table 2. Moreover, the two-parameter Ostwald–de Waele model has been used to govern the flow of this non-Newtonian shear thinning nanofluid.
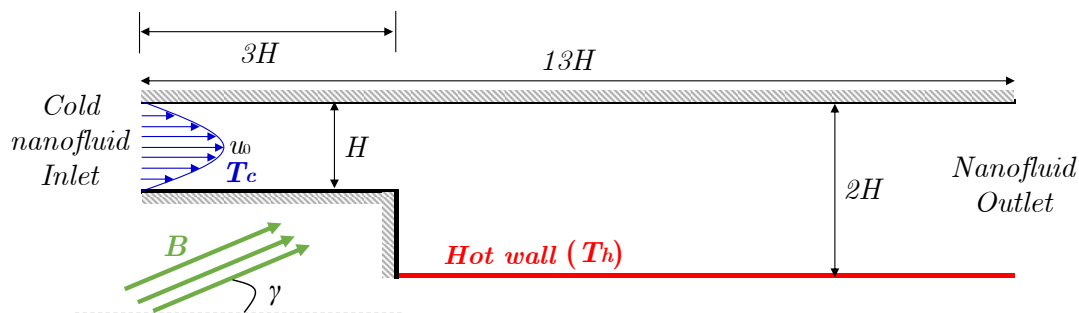
Figure 1. Backward Facing Step geometry

Table 1. Thermophysical proprieties of the nanoparticles and the base fluid.

Properties	Density [kg/m^3]	Thermal capacity [J/(kg.K)]	Thermal conductivity [W/(m.K)]	Dynamic viscosity [kg/(m.s)]	Thermal expansion [10^{-5}.1/K]	Electrical conductivity [S/K]
Eau (f)	997.1	4179	0.613	0.001003	21	0.05
CuO(p)	6500	540	18	-	0.85	2.7×10^{-8}

2.1. Mathematical model

The Navier-Stokes and heat equations are used to describe the flow of the non-Newtonian nanofluid flowing inside the BFS in a laminar regime. Let *x*, *y* be the Cartesian coordinates, *u*, *v* the

velocities along the x and y axis respectively, p the pressure of the nanofluid, T the temperature and τ the shear stress rate. The governing equations are:

$$\frac{\partial u}{\partial x} + \frac{\partial v}{\partial y} = 0 \tag{1}$$

$$\rho_{nf}\left(u\frac{\partial u}{\partial x} + v\frac{\partial u}{\partial y}\right) = -\frac{\partial p}{\partial x} + \left(\frac{\partial \tau_{xx}}{\partial x} + \frac{\partial \tau_{xy}}{\partial y}\right) + \sigma_{nf}B^2(v\cos\gamma\sin\gamma - u\sin\gamma) \tag{2}$$

$$\rho_{nf}\left(u\frac{\partial v}{\partial x} + v\frac{\partial v}{\partial y}\right) = -\frac{\partial p}{\partial y} + \left(\frac{\partial \tau_{yx}}{\partial x} + \frac{\partial \tau_{yy}}{\partial y}\right) + \sigma_{nf}B_0^2(u\cos\gamma\sin\gamma - v\cos\gamma) \tag{3}$$

$$\rho_{nf}Cp_{nf}\left(u\frac{\partial T}{\partial x} + v\frac{\partial T}{\partial y}\right) = k_{nf}\left(\frac{\partial^2 T}{\partial x^2} + \frac{\partial^2 T}{\partial y^2}\right) \tag{4}$$

where ρ, μ, k and Cp represents respectively the density, the dynamic viscosity, the heat conductivity and the specific heat, and the subscript "nf" denotes the nanofluid. The dynamic viscosity of the nanofluid is given as a function of the shear stress rate as follows:

$$\mu_{nf} = m_{nf}\left[2\left(\frac{\partial u}{\partial x}\right)^2 + 2\left(\frac{\partial v}{\partial y}\right)^2 + \left(\frac{\partial u}{\partial y} + \frac{\partial v}{\partial x}\right)^2\right]^{n_{nf}-1} \tag{5}$$

The nanofluid shear stress is given by:

$$\tau_{ij} = \mu_{nf}\left(\frac{\partial u_i}{\partial x_j} + \frac{\partial u_j}{\partial x_i}\right) \tag{6}$$

Let us introduce the Reynolds and Hartmann number, namely:

$$\mathrm{Re} = \frac{\rho_f U_0^{2-n_{nf}} H^{n_{nf}}}{m_f} \text{ and } Ha = BH\sqrt{\frac{\sigma_f}{\mu_f}} \tag{7}$$

Table 2. Value of the nanofluid consistency and behavior index (m, n) Santra et al. (2009).

Volume fraction (%)	Consistency (N.s^n.m^{-2})	Behavior index (-)
0.5	0.00187	0.880
1.0	0.00230	0.830
1.5	0.00283	0.780
2.0	0.00347	0.730
2.5	0.00426	0.680
3.0	0.00535	0.625
3.5	0.00641	0.580
4.0	0.00750	0.540
4.5	0.00876	0.500
5.0	0.01020	0.460

In Eq.(7), m_f is taken as the dynamic viscosity of the base fluid (0.001 Pa s). The other thermophysical proprieties of the nanofluid, i.e. density, thermal conductivity, specific heat and electrical conductivity, are calculated as function of the properties of nanoparticles (p) and base fluid (f) as:

$$\rho_{nf} = \varphi\rho_p + (1-\varphi)\rho_f \tag{8}$$

$$\frac{k_{\mathrm{nf}}}{k_{\mathrm{f}}} = \frac{k_{\mathrm{p}} + 2k_{\mathrm{f}} - 2\varphi(k_{\mathrm{f}} - k_{\mathrm{p}})}{k_{\mathrm{p}} + 2k_{\mathrm{f}} + \varphi(k_{\mathrm{f}} - k_{\mathrm{p}})} \tag{9}$$

$$(\rho Cp)_{\mathrm{nf}} = \varphi(\rho Cp)_{\mathrm{p}} + (1 - \varphi)(\rho Cp)_{\mathrm{f}} \tag{10}$$

$$\sigma_{\mathrm{nf}} = \varphi\sigma_{p} + (1 - \varphi)\sigma_{\mathrm{f}} \tag{11}$$

The boundary conditions used in this study are given as follows:

$$\text{Inlet: } u = U_{0}\left[-4\left(\frac{y}{H}\right)^{2} + 4\left(\frac{y}{H}\right)\right], \; v = 0 \text{ and } T = T_{c} \tag{12}$$

$$\text{Outlet: } p = 0 \text{ and } \frac{\partial T}{\partial x} = 0 \tag{13}$$

$$\text{Hot wall: } u = v = 0 \text{ and } T = T_{h} \tag{14}$$

$$\text{Other walls: } u = v = 0 \text{ and } \frac{\partial T}{\partial N} = 0 \tag{15}$$

The Nusselt number is calculated along the hot wall as follows:

$$\mathrm{Nu}_{l} = -\frac{k_{nf}}{k_{f}}\frac{H}{T_{h} - T_{c}}\left(\frac{\partial T}{\partial y}\right)_{\mathrm{hot \; wall}} \tag{16}$$

The average Nusselt number at this wall is given by:

$$\mathrm{Nu} = \frac{1}{10H}\int_{hot \; wall} Nu \; \mathrm{d}x \tag{17}$$

3. Numerical solution

The numerical resolution of the physical problem has been performed by using a finite element method based on the Galerkin discretization under Comsol Multiphysics 6.0 Software. The computational domain has been discretized with an unstructured triangular mesh. Moreover, close to the BFS walls, a rectangular boundary layer mesh has been introduced. After several trials of the mesh test for all the cases studied, we have opted for a grid with 134956 elements beyond which the values of the average Nusselt number remain unchanged.

4. Results and discussion

In this section, we examine the influence of Hartmann number, magnetic field angle, and nanoparticle volume concentration on heat transfer and vortex development within the backward facing step (BFS). The results are presented in the form of temperature contours, stream function contours, and local Nusselt number graphs along the hot wall.
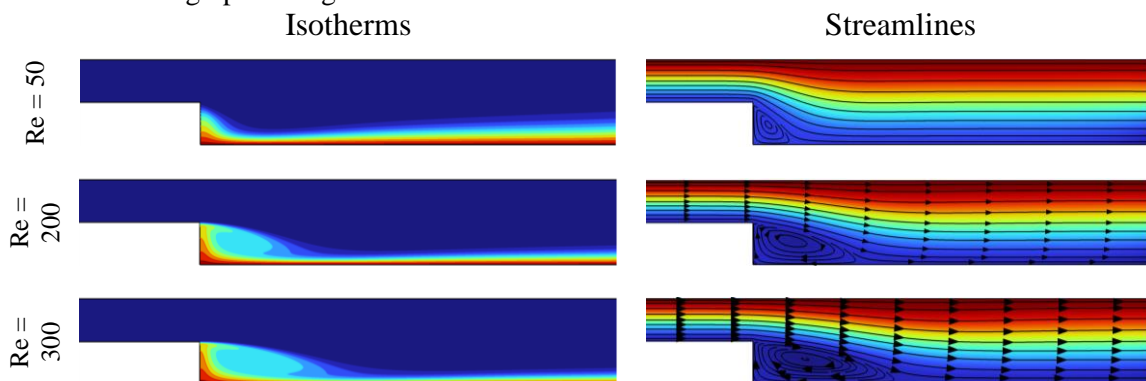
Figure 2. Isotherms and streamlines for different Reynolds numbers.
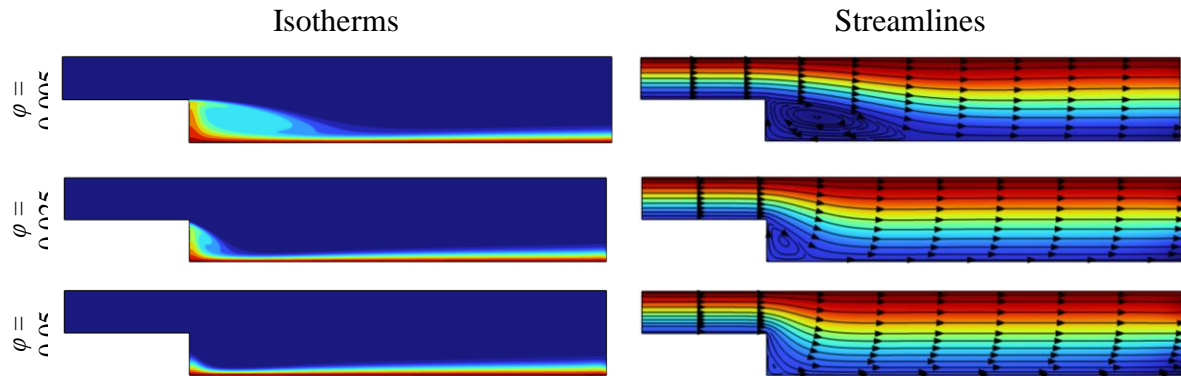
Figure 3. Isotherms and streamlines for different nanoparticle volume fraction.
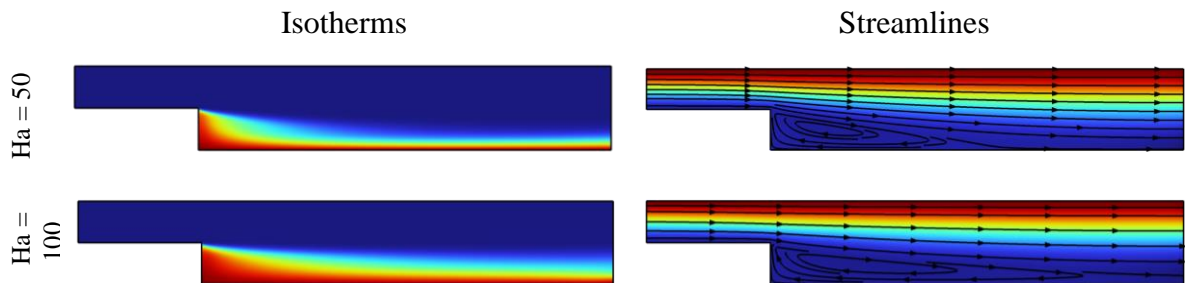
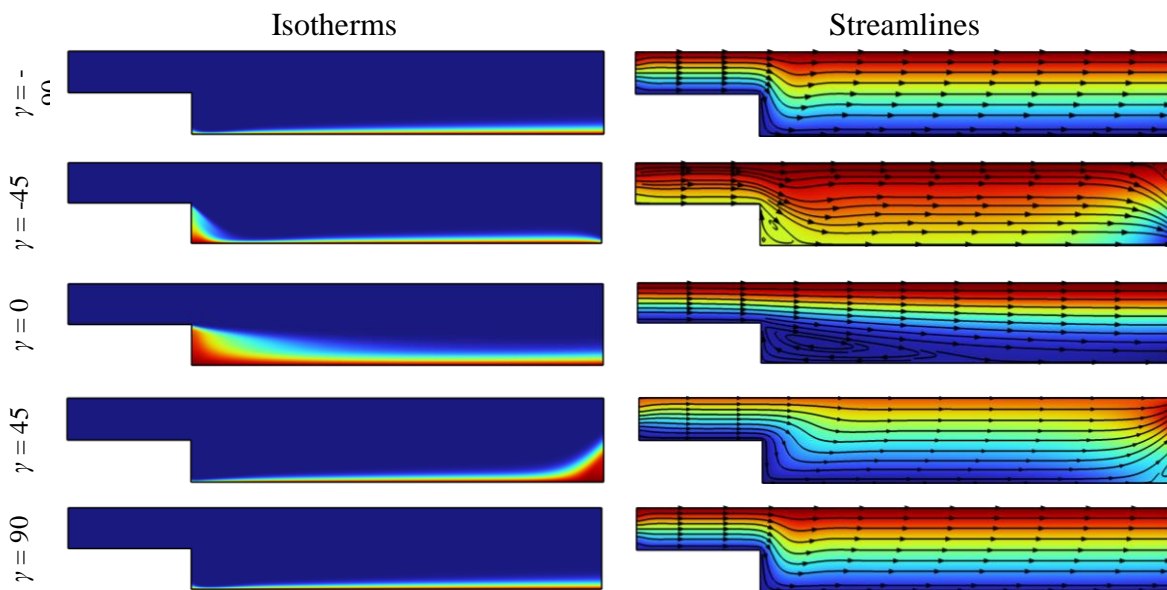**Figure 4.** Isotherms and streamlines for Ha=50 and Ha=100.

In Figure 2, the temperature distribution and the streamlines of the non-Newtonian nanofluid inside the downward step are reported for different Reynolds numbers. With increasing values of Re, the vortex zone expands while the thermal boundary layer decreases in size. Indeed, the thickness of the boundary layer decreases along the hot wall with increasing Re, except in the vortex region where an increase in the thickness of the boundary layer is observed. As an explication, as Re increases, inertial forces become dominant compared to viscous forces. This leads to an intensification of the laminar flow and an immediate flow reattachment downstream of the expansion zone. In the vortex region, the vortices generated by the flow result in an increase in the thickness of the thermal boundary layer. However, outside of this region, turbulent flow promotes heat dispersion and leads to a decrease in the thickness of the thermal boundary layer along the hot wall.

The impact of volume fraction on the flow of non-Newtonian nanofluid inside the BFS is shown in Figure 3. The influence of volume fraction of nanoparticles, which leads to the shear thinning behavior of the nanofluid, coincides with the influence of the structural index and consistency of the nanofluid, especially with the increase in its apparent dynamic viscosity. However, unlike the case of using the Newtonian single-phase model for nanofluids, the influence of volume fraction on the flow in the case of non-Newtonian nanofluid is clear and significant. Indeed, a considerable reduction in the flow was observed with increasing volume fraction of nanoparticles. Furthermore, the size of the vortex zone decreases significantly with increasing volume fraction, also leading to a decrease in the thermal boundary layer in the vortex region. These observations suggest that the addition of nanoparticles in the non-Newtonian nanofluid can disrupt the formation and stability of vortices, thereby reducing the size of the vortex zone.

The effect of a horizontal magnetic field on the flow and heat transfer of the shear thinning nanofluid is shown in Figure 4. Contrary to expectations, increasing the Hartmann number results in a significant reduction in the flow intensity of the nanofluid. However, this reduction in flow does not lead to the disappearance of the vortex zone, but rather to its substantial longitudinal expansion and thus to a significant increase in the thickness of the thermal boundary layer along the hot wall.

The effect of the magnetic field angle on the hydrodynamic and thermal behavior of the nanofluid inside the BFS is illustrated in Figure 5, with a reference angle of 0°. The figure shows that introducing a magnetic field with a different angle than 0° leads to an intensification of the flow. Moreover, the vortex zone is completely eliminated for angles of −90° and 90°, due to the interplay between the Lorentz force and the direction of the velocity field, which occurs specifically for these two angles. A decrease in the thickness of the thermal boundary layer is observed when the magnetic field inclination angle deviates from the horizontal position, particularly as it approaches angles of 90° and −90°. Furthermore, for γ= 45°, a slight increase in the thickness of this layer was observed near the outlet while for γ= −45° the thickness of the boundary layer is larger near the expansion zone.


Figure 5. Isotherms and streamlines for different magnetic field inclination angle.

In Figure 6, the local Nusselt number along the hot wall is reported for different for different values of the Reynolds numbers (a), nanoparticles volume fraction (b), Hartmann number (c), magnetic field inclination angle (d). Regarding the effect of Re, the figure shows that the Nusselt number increases along the hot wall until it reaches a maximum corresponding to the limit of the vortex zone. Beyond this zone, the Nusselt number starts to decrease. The increase in the Nusselt number along the hot wall is due to improved convective heat transfer. With increasing Re the flow becomes more intense, promoting better thermal dispersion and more efficient heat exchange with the hot wall. Vortices tend to disturb the thermal boundary layer, thereby reducing convective heat transfer near the hot wall. Therefore, despite the increase in Reynolds number, the presence of the vortex limits the continuous rise of the Nusselt number in this zone. Despite the negative impact of increasing Reynolds number on heat transfer in the vortex region, the overall convective heat transfer is significantly improved. Examining the average Nusselt number data presented in Table 3 (a), we observe a significant increase in the heat transfer rate with increasing Reynolds number. In particular, an enhancement percentage of 73% was observed at a Reynolds number of 300 compared to 50.

Concerning Figure 6(b), i.e. the variation of the local Nusselt number as a function of the volume fraction of CuO nanoparticles, increasing the volume fraction leads to a significant increase in the Nusselt number in the vortex zone, due to the dominant inertial and viscous effects in this region. However, outside the vortex zone a relatively small decrease in Nu is noted. The average Nusselt number presented in Table 3(b) increases up to 17% for a volume fraction of 0.05 of CuO nanoparticles, compared to a volume fraction of 0.005. Indeed, the addition of CuO nanoparticles leads to a significant improvement in the average heat transfer rate.

Figure 6(c) highlights the local variations of Nu along the hot wall, as a function of Ha, showing that in the considered measurement direction increasing Ha leads to a substantial reduction in the heat transfer rate. Furthermore, a decrease of approximately 68% in the average Nusselt number for Ha=100 is noted in Table Table 3 (c), compared to the case where no magnetic field is present (Ha = 0). This decrease is attributed to the magnetic forces acting on the movement of the nanofluid, thus limiting convection and heat transfer.

Figure 6(d) depicts the variation of the local Nusselt number along the hot wall as a function of different magnetic field inclination angles. According to this figure, angles different from 0° resulted in significantly higher heat transfer rates: angles of 45°, 90° and -90° exhibited the best convective heat transfer rates. Although the magnetic field hinders thermal activity, its angle has a positive impact: the heat transfer associated with angles of 90° and -90° (which are equivalent) showed the highest rate. An increase of approximately 203% was observed compared to the case of a horizontal magnetic field. Non-zero inclination angles significantly improve the convective heat transfer rate along the hot wall, see Table 3(d).
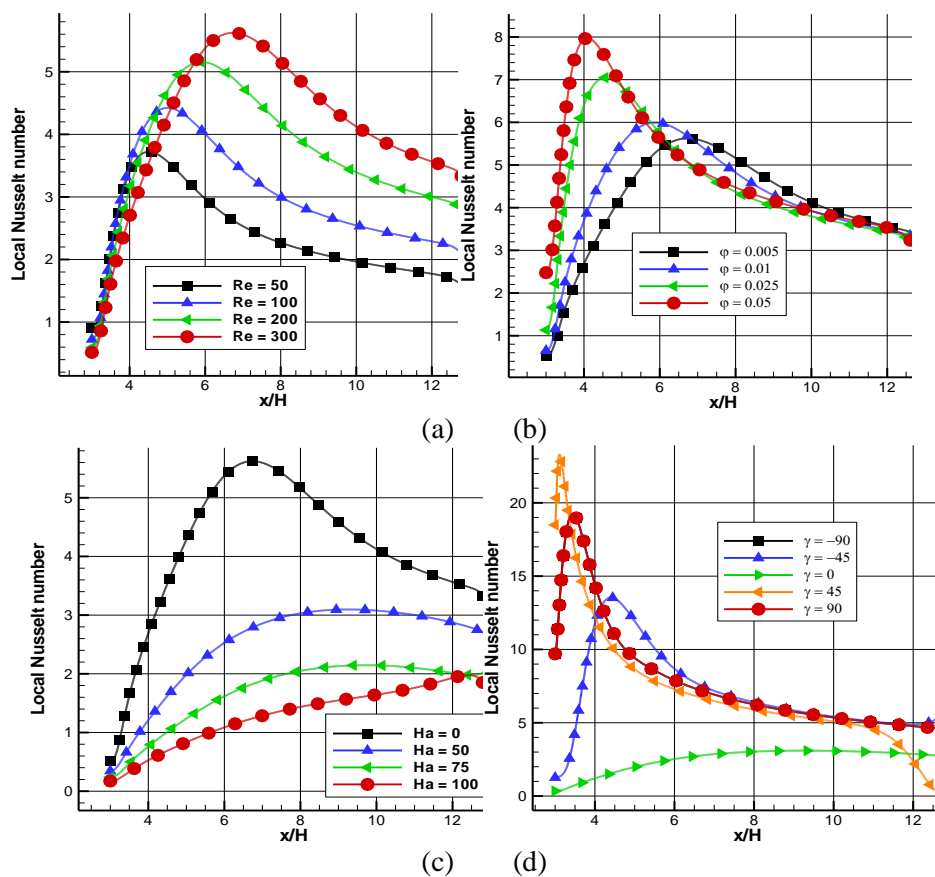
Figure 6. Local Nusselt number for different values of Reynolds numbers (a), nano-particle volume fraction (b), Hartmann number (c), magnetic field inclination angle (d).

5. Conclusion

This paper investigated the hydrodynamic and thermal behavior of non-Newtonian nanofluid flow inside a backward-facing step (BFS) under various influencing factors. The findings shed light on the intricate interplay between flow characteristics, heat transfer, and the presence of magnetic fields in the BFS domain. The main findings can be summarized as follows.

- As the Reynolds number increases, the vortex zone expands while the thermal boundary layer thickness along the hot wall decreases, except within the vortex region where it increases.

- An increase in nanoparticle volume fraction leads to a considerable reduction in flow intensity and vortex size, as well as to a decrease in the thermal boundary layer in the vortex region: the addition of nanoparticles disrupts the formation and stability of vortices.
- Surprisingly, an increase in the Hartmann number resulted in a significant reduction in flow intensity. However, the vortex zone was not eliminated but rather longitudinally expanded, leading to an increase in the thermal boundary layer thickness along the hot wall.
- The complete elimination of the vortex zone was observed at angles of −90° and 90°, probably due to the interaction between the Lorentz force and the velocity field direction. Moreover, changes in the thermal boundary layer thickness were observed as the inclination angle deviated from the horizontal position: angles of 45°, 90° and −90° exhibited the highest convective heat transfer rates.

Table 3. Average Nusselt number for different values of the Reynolds number (a), nanoparticle volume fraction (b), Hartmann number (c), magnetic field inclination angle (d).

(a)	Re	50	100	200	300
	Nu_{ave}	2.377	2.990	3.700	4.124
	% Heat rate	-	73.45	55.64	73.45
(b)	φ	0.005	0.010	0.025	0.050
	Nu_{ave}	4.124	4.301	4.567	4.846
	% heat rate	-	4.29	10.73	17.51
(c)	Ha	0	50	75	100
	Nu_{ave}	4.124	2.523	1.708	1.307
	% heat rate	-	-38.81	-58.57	-68.29

	γ	0	-90	90	-45	45
(d)	Nu_{ave}	2.523	7.668	7.668	6.868	7.050
	% heat rate	-	203.8	203.8	172.1	179.3

References

[1] Eturk E 2008 Numerical solutions of 2-D steady incompressible flow over a backward-facing step, Part I: High Reynolds number solutions *Comput Fluids* **37** 633-655

[2] Lan H, Armaly B F, Drallmeier J A 2009 Three-dimensional simulation of turbulent forced convection in a duct with backward-facing step *Int J Heat Mass Transf* **52** 1690-1700

[3] Iwai H, Nakabe K, Suzuki K 2000 Flow and heat transfer characteristics of backward-facing step laminar flow in a rectangular duct *Int J Heat Mass Transf* **43** 457-471

[4] Star S, Stabile G, Rozza G, Degroote J 2021 A POD-Galerkin reduced order model of a turbulent convective buoyant flow of sodium over a backward-facing step *Appl Math Model*, **89** 486-503

[5] Mahmood R, Bilal S, Majeed A H, Khan I., Sherif E S M 2020 A comparative analysis of flow features of Newtonian and power law material: a new configuration *J Mater Res Technol* **9** 1978

[6] Barletta A, Rossi di Schio E, Celli M 2015 Convection and instability phenomena in nano-fluid-saturated porous media *Heat Transfer Enhancement with Nanofluids* CRC Press FL 341-364

[7] Rossi di Schio E, Impiombato A N, Mokhefi A, Biserni C 2022 Theoretical and Numerical Study on Buongiorno's Model with a Couette Flow of a Nanofluid in a Channel with an Embedded Cavity *Appl Sci* **12** 7751.

[8] Selimefendigil F and Öztop H F 2013 Identification of forced convection in pulsating flow at a backward facing step with a stationary cylinder subjected to nanofluid *Int Commun Heat Mass Transf* **45** 111-121

[9] Selimefendigil F and Öztop H F 2013b Numerical analysis of laminar pulsating flow at a backward facing step with an upper wall mounted adiabatic thin fin *Comput Fluids* **88** 93-107

[10] Selimefendigil F and Öztop H F 2017 Forced convection and thermal predictions of pulsating nanofluid flow over a backward facing step with a corrugated bottom wall *Int J Heat Mass Transf* **110** 231-247